Application of Immersional Calorimetry to Investigation of Solid–Liquid Interactions: Microcrystalline Cellulose–Water System

R. GARY HOLLENBECK *, GARNET E. PECK, and DANE O. KILDSIG ˣ

Abstract ☐ A comprehensive characterization of the specific solid–liquid interaction for microcrystalline cellulose and water is presented. The procedure consisted of a conjoint vapor adsorption and immersional wetting experiment. The following information was obtained with respect to the solid. Estimates of the total surface area ($138 \ m^2/g$) and the external surface ($9.2 \ m^2/g$) were calculated from the adsorption and immersion data, respectively. Existence of an energetically homogeneous surface was verified by a linear decrease in the heat of immersion of samples containing adsorbed moisture approximately up to monolayer capacity. Integral and differential free energy, enthalpy, and entropy changes accompanying the adsorption process were calculated, and a lack of swelling was substantiated by comparison with a similar study of cellulose fibers. Immersional hysteresis was observed, and its magnitude suggested that sorption hysteresis was of enthalpic as well as entropic origin. The experimental method is potentially valuable for routine characterization of hydrophilic powders.

Keyphrases ☐ Solid–liquid interactions—microcrystalline cellulose–water system characterized, immersional calorimetry–vapor adsorption procedure ☐ Cellulose, microcrystalline–water system—solid–liquid interactions characterized by immersional calorimetry–vapor adsorption procedure ☐ Calorimetry, immersional—combined with vapor adsorption procedure to characterize solid–liquid interactions of microcrystalline cellulose–water system ☐ Adsorption, vapor—combined with immersional calorimetry procedure to characterize solid–liquid interactions of microcrystalline cellulose–water system

Most problems encountered in the production and performance of solid and liquid dosage forms can be resolved in terms of solid–liquid interactions. The basis for an experimental characterization of these interactions (1) involved the confluence of immersional calorimetry and vapor adsorption. The combination of these two powerful techniques has been used to describe the wetting of hydrophilic and hydrophobic solids (1–12).

This study represents a comprehensive investigation of the specific solid–liquid interaction for microcrystalline cellulose and water.

THEORETICAL

The thermodynamics of wetting deal with the entire spectrum of solid–liquid interactions, ranging from the adsorption of a small amount of vapor by a relatively large amount of solid to the immersion of a small quantity of solid into a large amount of liquid. Both the adsorption and immersion processes involve the same fundamental interactions; they differ only in the relative amounts of each component. An experimental investigation involving both of these processes can provide a complete characterization of the mutual affinity of the solid and liquid.

Free Energy Changes—At constant temperature, the net integral free energy change, ΔF, associated with the adsorption of a volatile liquid (Component 1) on a nonvolatile solid (Component 2) is given as:

$$\Delta F = \overline{\Delta F_1} n_1 + \overline{\Delta F_2} n_2 \qquad \text{(Eq. 1)}$$

where $\overline{\Delta F_1}$ and $\overline{\Delta F_2}$ are the partial molal free energy changes of the volatile and nonvolatile components, respectively; and n_1 and n_2 are the numbers of moles of each, respectively.

Since the adsorption process is most often regarded with respect to the thermodynamic characteristics of the volatile component, $\overline{\Delta F_1}$ is referred to simply as the differential free energy change of adsorption. The equilibrium adsorption isotherm provides the information necessary to determine both the differential and integral free energy changes.

The differential free energy change is given as the difference between the chemical potential of liquid in the adsorbed state and pure liquid:

$$\overline{\Delta F_1} = u_1 - u_1{}^0 = RT \ln P/P_0 \qquad \text{(Eq. 2)}$$

where u_1 and $u_1{}^0$ are the chemical potentials of the adsorbate and pure liquid, respectively; P is the actual vapor pressure; P_0 is the vapor pressure of pure liquid at experimental temperature T; and R is the gas constant.

With a form of the Gibbs–Duhem relation:

$$\overline{\Delta F_2} = \int - (n_1/n_2) \, d \, \overline{\Delta F_1} \qquad \text{(Eq. 3)}$$

an expression for the integral free energy change can be obtained. By substitution of the partial molal equalities of Eqs. 2 and 3 into Eq. 1, the integral free energy change is obtained as:

$$\Delta F = n_1 RT \ln P/P_0 - RT \int n_1 \, d \ln P/P_0 \qquad \text{(Eq. 4)}$$

Equations 2 and 4 were presented explicitly by Dole and McLaren (13).

Evaluation of the integral on the right-hand side of Eq. 4 can be performed graphically from a plot of $n_1 P_0/P$ versus P/P_0, recognizing the identity:

$$-RT \int_0^{P/P_0} n_1 \, d \ln \left(\frac{P}{P_0}\right) \equiv -RT \int_0^{P/P_0} \frac{n_1 P_0}{P} d\left(\frac{P}{P_0}\right) \qquad \text{(Eq. 5)}$$

Errors associated with low pressure extrapolation to $P = 0$ are smaller with this technique than with a plot of n_1 versus $\ln P/P_0$.

The differential free energy change has units of energy per mole of adsorbate, because it refers to the volatile component. The integral free energy change simply has units of energy, because the entire process is specified for a certain number of moles of each component.

Enthalpy Changes—Figure 1 is a pictorial representation of the interrelationship between the various enthalpy changes associated with the wetting of a solid by a liquid. Step 1 represents the immersion of a dry solid into a large quantity of liquid. The enthalpy change associated with this process is referred to as the "heat of immersion of the dry solid" and is designated $\Delta H_i(S/L)$, the parenthetical S/L indicating the process of going from a clean solid to a solid–liquid interface (3).

Step 4 also represents an immersional process, only now the solid contains adsorbed moisture. The heat of immersion of this wet solid is designated $\Delta H_i(S_f/L)$, where the f indicates that the solid possesses a "film" of adsorbed liquid (3). The value of $\Delta H_i(S_f/L)$ depends on the number of moles of water adsorbed, n_1.

The final states of Steps 1 and 4 are identical, and the enthalpy change associated with Step 1 is clearly equivalent to the sum of Steps 2–4:

$$\Delta H_i(S/L) = n_1 \lambda + \Delta H(\text{ads}) + \Delta H_i(S_f/L) \qquad \text{(Eq. 6)}$$

where λ is the molar heat of vaporization of the liquid and $\Delta H(\text{ads})$ is the heat of adsorption.

The net integral enthalpy change associated with the adsorption process, ΔH, is the heat change in excess of the normal condensation of the liquid:

$$\Delta H = \Delta H(\text{ads}) - (-n_1 \lambda) \qquad \text{(Eq. 7)}$$

Therefore, from Eq. 6:

$$\Delta H = \Delta H_i(S/L) - \Delta H_i(S_f/L) \qquad \text{(Eq. 8)}$$

Table I—Initial Conditions of Relative Humidity Chambers at 25°

Chamber	H_2SO_4, % (w/w)	Relative Humidity, %
1	68.79	5.75
2	63.87	10.75
3	59.16	18.00
4	55.30	24.75
5	52.20	30.50
6	43.48	48.75
7	33.16	70.00
8	25.44	81.50
9	17.61	90.25
10	—	100.00

The integral enthalpy change once again has units of energy; by measuring the heats of immersion of solids with varying moisture contents, the entire range of ΔH values can be obtained.

The partial molal enthalpy change with respect to the volatile component, $\overline{\Delta H_1}$, can easily be obtained by estimating the slope of the ΔH versus n_1 curve, where the data have been normalized for a constant amount of solid. This thermodynamic quantity is often referred to as the differential heat of adsorption and has units of energy per mole of adsorbate.

Where swelling of the solid occurs, the integral and differential enthalpies of adsorption calculated through an immersional procedure are influenced by the endothermic swelling term. The effect is a decrease in both thermodynamic quantities.

Entropy Changes—Both the integral and differential entropy changes can be obtained from the defining equations once the other thermodynamic variables are determined:

$$\Delta S = (\Delta H - \Delta F)/T \qquad \text{(Eq. 9)}$$

$$\overline{\Delta S_1} = (\overline{\Delta H_1} - \overline{\Delta F_1})/T \qquad \text{(Eq. 10)}$$

Surface Area Analysis—Both adsorption and immersion data can be used to estimate a surface area relative to the solid. In adsorption studies, the surface area calculated is the area accessible to adsorption by the adsorbate. In an immersion study, the area represents the area of a film of liquid on the solid particle.

The constant-temperature adsorption data are generally analyzed using the linear form of the Brunauer, Emmett, and Teller (BET) equation (14, 15):

$$\frac{P/P_0}{v(1 - P/P_0)} = \frac{1}{cv_m} + \frac{(c - 1)}{cv_m}(P/P_0) \qquad \text{(Eq. 11)}$$

where P/P_0 is the relative vapor pressure, v is the amount of gas adsorbed at P/P_0, and v_m and c are parameters of the equation.

The value of v_m is used as an estimate of the monolayer capacity, so the solid surface area can be calculated from the known area of one adsorbate molecule. In these experiments, values of 16.2 and 12.5 A^2 were used as the molecular areas of nitrogen and water, respectively.

The parameter c is related by theory to the average energy of adsorption:

$$c = e^{-(\Delta E/RT)} = e^{-(E_1 - E_L)} \qquad \text{(Eq. 12)}$$

where E is the net energy of adsorption, E_1 is the energy of adsorption of the first layer of adsorbate, and E_L is the energy of liquefaction of the adsorbate.

A second estimate of the surface area can be obtained through application of the "absolute" method of Harkins and Jura (16). This method is based on the immersion of samples equilibrated at $P/P_0 = 1$. These samples are assumed to be covered with liquid to the extent that the film-covered surface has an enthalpy not unlike that of pure liquid. Therefore, the immersion of the film-covered sample results in the release of a quantity of heat directly proportional to the surface area of the film destroyed.

From surface tension measurements, the heat content of pure liquid water was determined to be 118 ergs/cm². By using the heat of immersion of the solid equilibrated at 100% relative humidity (RH), the surface area, A, is given by:

$$A = \frac{\Delta H_i(S_f/L)^*}{118 \text{ ergs/cm}^2} \qquad \text{(Eq. 13)}$$

where $\Delta H_i(S_f/L)^*$ is the heat of immersion of the sample equilibrated at 100% RH expressed in ergs per amount of solid. The surface area obtained in this manner is an estimate of the "external" surface area of the
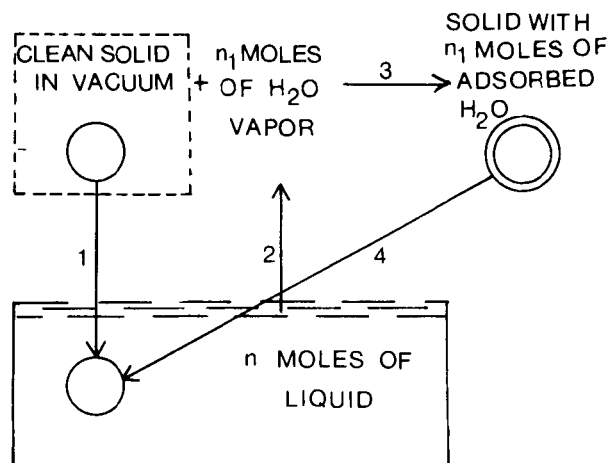

Figure 1—*Relationship between adsorption and immersion (adapted from Ref. 3).*

solid material since the capillaries and some intra-aggregate spaces are filled with water.

EXPERIMENTAL

Microcrystalline cellulose[1], dried at approximately 70° in a vacuum oven (= 0.1 mm Hg) for 24 hr, was used as the starting material in all experiments. The average moisture content of the dried material was measured gravimetrically by further drying at 100° and determined to be about 0.2% on a dry weight basis. This value was based on two independent determinations; the solid turned brown at elevated temperature (100°).

A water vapor sorption study was performed to obtain a complete adsorption–desorption isotherm as well as to generate samples with varying moisture contents. Equilibrated samples were subsequently used in an immersional study.

For comparative purposes, a low pressure nitrogen adsorption isotherm was also obtained and analyzed as an independent estimate of the surface area.

Water Vapor Sorption—Relative humidity chambers, varying from 5 to 100% RH, were prepared. Glass[2] containers, normally used as desiccators, were employed as chambers; the relative humidity was controlled by using sulfuric acid solutions of varying concentration, based upon the relationship established by Stokes and Robinson (17). Actual concentrations of sulfuric acid were determined by titrating aliquots of the final solutions with standardized sodium hydroxide. Table I contains the initial conditions obtained for each chamber.

Water adsorption was followed by a simple gravimetric method. Two previously weighed containers were filled with dry powder, weighed, and placed in each chamber. For these experiments, 60 × 15-mm petri dish[3] tops were used as containers.

All weighings were performed on an analytical balance[4] with a resolution of ±0.1 mg. Initial sample weights, from approximately 4.5 to 7.0 g, were determined by difference. Subsequent weighings were made at 3, 4, and 7 days. Humidity chambers were stored in a constant-temperature room maintained at 25 ± 0.5°.

Desorption studies were performed in essentially the same manner with samples equilibrated at 100% RH for 1 week. Weight determinations were made at 5, 7, and 8 days.

Nitrogen Adsorption—A commercially available apparatus[5] was employed to obtain a nitrogen adsorption isotherm at low relative pressures. The microcrystalline cellulose sample was degassed until the rate of pressure increase in the closed system (not exposed to vacuum) was less than 0.0001 mm Hg/min at room temperature. Adsorption data were generated at 77 °K by sequential addition in such a manner that six data points were obtained in the relative pressure range of 0.05–0.35.

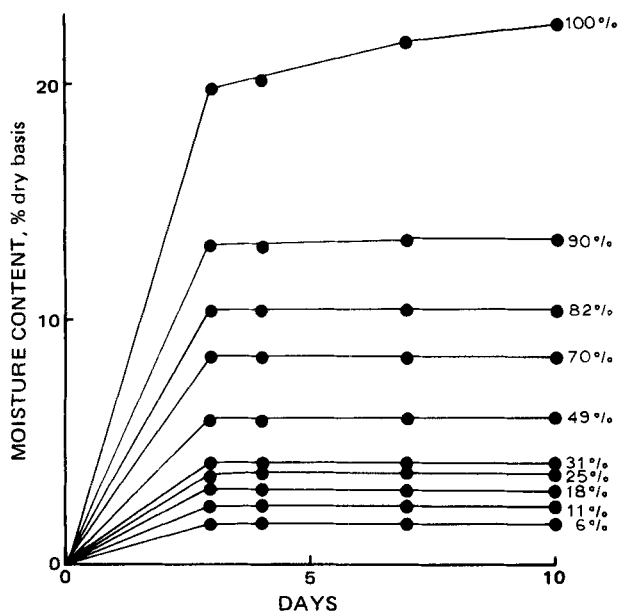**Aqueous Immersional Calorimetry**—Heats of immersion of mi-

Figure 2—*Adsorption of water by microcrystalline cellulose at various relative humidities.*

crocrystalline cellulose containing various amounts of adsorbed water and water remaining after the desorption process were determined in a nonisothermal calorimeter (18). The design of this calorimeter and aspects of its operation were presented previously (19).

A thin-walled glass sample bulb was tared and partially filled with powder equilibrated under one of the previously described conditions. The weight of the sample was obtained by the difference between the filled and empty sample bulbs.

The calorimeter cell was filled with an accurately measured quantity of distilled water (either 200 or 250 ml), and the entire unit was assembled. Stirring was initiated, and the temperature of the calorimeter contents, θ, was adjusted to approximately 25° by actuation of the calibration heater.

Thermal equilibration of the system was assumed complete when the observed $\Delta\theta/\Delta t$ values were not greater than ±0.0002°/interval. (The digital thermometer reports the temperature at 10-sec intervals when operated at a resolution of 0.0001°.) After stabilization, the recorder was turned on and a preprocess rating period of at least 5 min (30 intervals) was allowed. The sample bulb was then fractured by a rapid depression and release of the beaker rod.
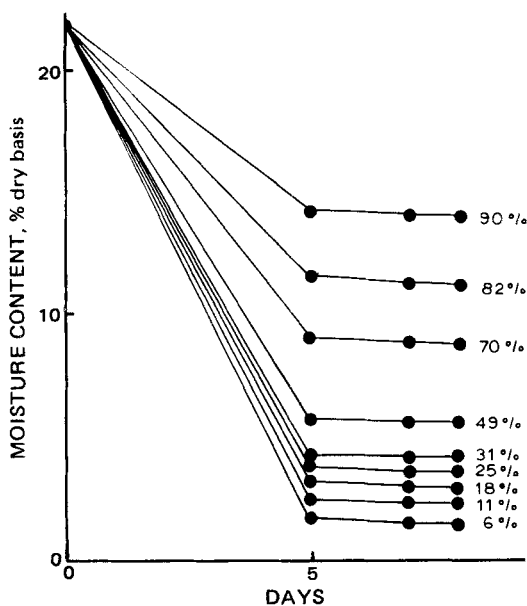

Figure 3—*Desorption of saturated microcrystalline cellulose at various relative humidities.*
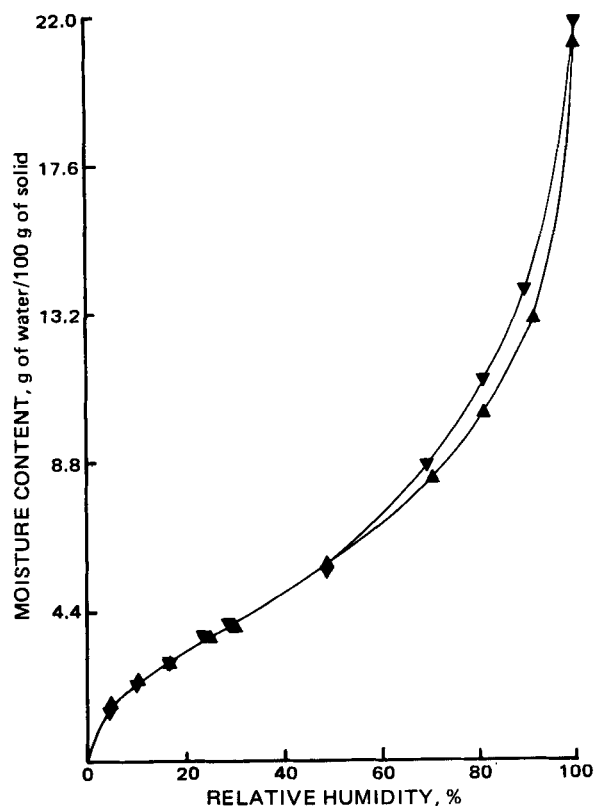

Figure 4—*Water vapor sorption isotherm for microcrystalline cellulose at 25°. Key: ▲, adsorption; and ▼, desorption.*

During the 5 min allowed after process initiation, the calibration heater power supply was stabilized by discharge through a 3-ohm external resistance circuit. A calibration was then accomplished by an actuation of the resistance heater in the calorimeter cell for approximately 10 sec, during which the voltage across the heater was measured. After termination of the heating process, the duration of the actuation was recorded.

A 5-min period was allowed before termination of the experiment. This procedure was employed for all samples.

Intrinsic temperature changes for the wetting and calibration processes were computed using the differential transformation method described previously (19). The heat capacity used to compute the heats of wetting was obtained by averaging the results of all calibrations within the same set of experiments. The accuracy of all heats of wetting is related to the accuracy of the heat capacity determination for the system (see Table III, Ref. 19). The accuracy of the heat capacity determinations is approximately ±0.6%.

Immersional experiments were performed in three sets; samples containing adsorbed water taken after 3 and 7 days of equilibration and samples containing water remaining after the 8-day desorption process.

RESULTS AND DISCUSSION

Water Vapor Sorption—Figures 2 and 3 represent the adsorption and desorption of water by dry microcrystalline cellulose and saturated microcrystalline cellulose, respectively. These processes occurred relatively fast, reaching virtual completion in 5 days or less for all samples, except the adsorption of water at 100% RH.

The equilibration adsorption–desorption isotherm is presented in Fig. 4. This isotherm is clearly a Type II, with a slight degree of hysteresis in the upper pressure region. The sorption hysteresis is shown for microcrystalline cellulose is classical for cellulosics, although its magnitude is considerably less than that for standard cellulose (11).

The etiology of sorption hysteresis in these systems was discussed previously (9, 11, 20–22). Gregg (22) stated that, in many cases, the phenomenon is due to a very slow rate of equilibrium attainment and, hence, is actually an artifact. His view considers that the desorption branch represents a kind of supersaturation effect and, if a long enough time is allowed, the hysteresis will disappear. There is some evidence in
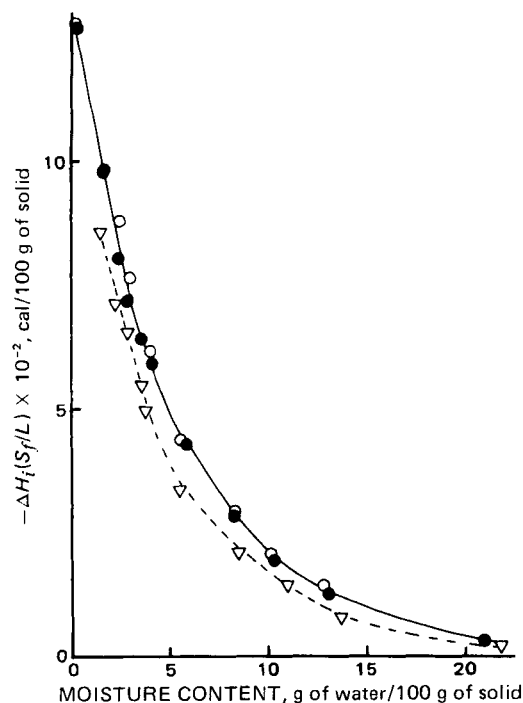
Figure 5—*Heats of wetting of microcrystalline cellulose containing various amounts of adsorbed and desorbed water. Key:* O, *samples equilibrated for 3 days at varying humidity (adsorption);* ●, *samples equilibrated for 7 days at varying humidity (adsorption); and* ▽, *samples equilibrated for 8 days at varying humidity (desorption).*

Figure 6—*BET plot for water vapor adsorption on microcrystalline cellulose where* v = *grams of water per gram of solid.*

this work with microcrystalline cellulose that the system may not be at equilibrium. At high relative humidities, the adsorption and desorption moisture contents may indeed be approaching each other at a very slow rate.

However, other thermodynamic evidence indicates that the hysteresis may be real. When the system is thermodynamically stable, the sorption hysteresis reflects a difference in the free energy of the two systems at the same relative pressure. It follows that the hysteresis may be due to a difference in specific surface area (irreversible swelling), solid–liquid bonding strengths (enthalpy effect), molecular ordering (entropy), or a combination of these effects. Therefore, a complete thermodynamic analysis can help identify the origin of the hysteresis. Such an analysis is presented in the following sections.

Heats of Immersion—Figure 5 represents the immersional isotherm for microcrystalline cellulose containing various amounts of adsorbed water and water remaining after the desorption process.

The initial region of the curve for solid containing adsorbed water demonstrates a nearly linear decrease in the heat of wetting as the moisture content increases. Zettlemoyer et al. (8) considered this type of relationship to be indicative of an energetically homogeneous surface. The heat evolved on wetting appears to depend simply on the amount of bare surface present. If there were a distribution of energy sites on the surface of the solid, the high energy sites would preferentially adsorb vapor molecules and the heat of immersion would not be proportional to the amount of surface but, instead, would depend on which sites were occupied.

The desorbed samples had heats of wetting consistently lower than the samples containing an equivalent amount of adsorbed water. Thus, a hysteresis of the immersional isotherm also exists.

Argue and Maass (20) also found an immersional hysteresis in the wetting of cellulose samples, but it was the opposite of that in Fig. 5; their desorbed samples exhibited the greater heats of wetting. Argue and Maass (20) concluded that this behavior was characteristic of a solid that swells irreversibly when immersed in water.

Swelling is an endothermic process involving the rupture of some solid–solid bonds. Their solid samples containing adsorbed water exhibited a lower heat of immersion than expected, because some of the energy released in wetting was consumed in the swelling process. Alternatively, the heat of immersion of solid with water remaining after desorption did not involve this endothermic term since the solid already had the opportunity to swell during its long exposure to 100% RH.
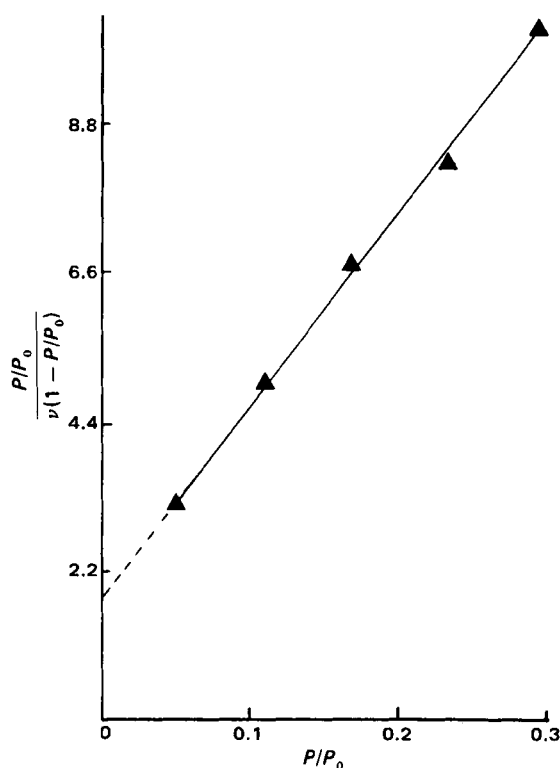
After desorption, the standard cellulose employed by Argue and Maass (20) had a higher specific surface area than the solid containing adsorbed water. This information is important in identifying the origin of sorption hysteresis.

Microcrystalline cellulose clearly does not show irreversible swelling. The sorption hysteresis for this solid cannot be explained on the basis of specific surface area changes.

Morrison and Dzieciuch (11) found no differences between the heats of wetting of adsorbed and partially desorbed cellulose samples containing equivalent amounts of water. The coincidental wetting curves indicate either no swelling or completely reversible swelling. In either event, since the enthalpies are the same for equivalent moisture contents, the sorption hysteresis is of entropic origin.

The observed hysteresis in the present study represents the final possibility: lower heats of wetting for the partially desorbed samples. Dunford and Morrison (9) found a similar, though smaller, hysteresis in their study involving silk fibroin. These authors remarked: "At equal moisture contents, water is more tightly held on the desorption branch. Therefore, we would expect the heat of wetting to be less for the desorption side if there are no phenomena occurring other than pure adsorption." Actually, this statement involves some circular reasoning; it may be better to emphasize that this type of immersional hysteresis stands as evidence that the water is "held" more tightly on the desorption branch of the isotherm than it is on the adsorption branch. For the microcrystalline cellulose–water system, the strength of the solid–liquid interaction plays a role in the production of sorption hysteresis. In a later section, the extent to which this role accounts for the entire phenomenon will be assessed by observing the relative changes in the enthalpy and entropy values.

Surface Area Analysis—Based on the information collected in this study, three independent estimates of the surface area of microcrystalline cellulose were obtained.

An analysis of the water vapor adsorption data indicated that the BET theory (14, 15) could be applied in the range of 5–30% RH. Figure 6 depicts the low pressure adsorption data when plotted using the linear form of the BET equation (Eq. 11). The monolayer capacity of 0.0330 g of water/g of solid obtained in this manner corresponds to a surface area of 138 m^2/g. A value of 149 m^2/g was obtained by Nakai et al. (23) in a similar study.

Figure 7 represents the results of the nitrogen adsorption study. With the BET theory for these data, a surface area of 1.5 m^2/g was estimated. Surface area measurements of 11.2 and 1.0 m^2/g were reported for mi-

Table II—Calculated Thermodynamic Properties for the Adsorption of Water on Microcrystalline Cellulose

$n_1{}^a$, moles of Water	P/P_0	$-\Delta H^*$, cal	$-\Delta F^*$, cal	$-\Delta S^*$, eu	$-\Delta \bar{H}$, cal/mole of Water	$-\Delta \bar{F}_1$, cal/mole of Water	$-\Delta \bar{S}$, eu/mole of Water
0.01	—	40	—	—	3750	—	—
0.02	—	75	—	—	3500	—	—
0.03	—	110	—	—	3500	—	—
0.04	—	145	—	—	3500	—	—
0.05	0.0216	180	147.2	0.11	3500	2271	4.12
0.06	0.0276	215	169.2	0.15	3500	2126	4.61
0.07	0.0343	250	190.0	0.20	3500	1997	5.04
0.08	0.0419	285	209.1	0.26	3500	1879	5.44
0.09	0.505	320	227.4	0.31	3500	1768	5.81
0.10	0.0602	355	244.6	0.37	3500	1664	6.16
0.11	0.075	390	260.6	0.43	3500	1534	6.60
0.12	0.088	425	275.4	0.50	3500	1439	6.92
0.13	0.105	460	289.3	0.57	3500	1335	7.27
0.14	0.120	495	302.3	0.65	3500	1255	7.53
0.15	0.135	530	314.5	0.72	3250	1186	8.32
0.16	0.152	560	326.0	0.79	3000	1115	6.33
0.17	0.170	590	336.8	0.85	3000	1049	6.55
0.18	0.195	620	347.0	0.92	2750	968	5.98
0.19	0.212	645	356.4	0.97	2400	918	4.97
0.20	0.235	668	365.2	1.02	2325	857	4.93
0.22	0.282	713	381.4	1.11	1925	750	3.94
0.24	0.330	745	395.5	1.17	1600	656	3.17
0.26	0.370	777	407.9	1.24	1575	589	3.31
0.28	0.410	808	419.1	1.31	1525	528	3.35
0.30	0.445	838	429.1	1.37	1450	479	3.26
0.32	0.480	866	438.3	1.44	1375	435	3.15
0.34	0.512	893	446.6	1.50	1275	396	2.95
0.36	0.542	917	454.2	1.55	1175	363	2.72
0.38	0.575	940	461.1	1.61	1150	328	2.76
0.40	0.605	963	467.3	1.66	1075	298	2.61
0.42	0.635	983	472.9	1.71	975	269	2.37
0.44	0.665	1002	478.1	1.76	925	242	2.29
0.46	0.690	1020	482.7	1.80	900	220	2.28
0.48	0.715	1038	486.9	1.85	900	199	2.35
0.50	0.738	1056	490.6	1.90	805	180	2.10
0.60	0.835	1124	504.9	2.08	560	107	1.52
0.70	0.897	1168	5i3.4	2.20	370	64	1.03
0.80	0.935	1198	518.6	2.28	260	40	0.74
0.90	0.967	1220	521.5	2.34	145	20	0.42
1.00	0.987	1237	523.0	2.40	—	—	—

^{a} With respect to 100 g of solid.

crocrystalline cellulose based on similar nitrogen adsorption studies (23, 24).

The difference between the size of the nitrogen and water molecules is not sufficient to account for the monumental difference observed in the results of these two methods. Young and Healey (6) observed a similar phenomenon in adsorption studies on asbestos. They showed that the source of the difference between nitrogen and water vapor adsorption studies is associated with the difficulty in removing water from a solid where it is held by strong capillary and adsorption forces. Residual water, which is likely a solid at the 77 °K used in the nitrogen adsorption study, occludes a significant amount of surface in the nitrogen study. In this sense, the surface area values determined should be quite sensitive to the sample pretreatment, so the variation in reported values is understandable.

It may be considered from this observation that nitrogen adsorption provides an estimate of the "external" area of the solid.

As indicated under *Theoretical*, the immersional data provide another estimate of the external area of the film-covered solid. A value for $\Delta H_i(S_fL)^*$ of 26 cal/100 g of solid was obtained from Fig. 5. With Eq. 13, a value of 9.2 m²/g was obtained for the area of microcrystalline cellulose.

Microcrystalline cellulose aggregates into clusters during spray drying (25). The low pressure analysis represented by the BET analysis provides an estimate of the total surface area of the microcrystals. Conversely, at the high relative moisture pressures used in the method of Harkins and Jura (16), the "internal" space of these aggregates is filled with water.

Following the analysis of Zettlemoyer *et al.* (8), the total surface of the aggregates is then 140–280 m²/g. The upper limit of this range comes from the consideration that if one layer of adsorbed water molecules occupies the space between two close layers of solid, the calculated surface area (approximately 140 m²/g) is actually only one-half of the total surface area. Also, considering an estimate of 10 m²/g for the external area, it appears that the internal surface area is 130–270 m²/g.

Thermodynamics of Adsorption—The smooth adsorption isotherm in Fig. 4 was used to calculate the differential, $\overline{\Delta F}_1$, and integral, ΔF, free energy changes associated with the adsorption of water by microcrystalline cellulose using Eqs. 2 and 4. The first two columns of Table II represent the coordinate moisture content and partial pressure values chosen at regular intervals from the adsorption branch of the isotherm in Fig. 4. The calculated integral and differential free energies are found in columns 4 and 7 of Table II, respectively.

The integral and differential enthalpy changes associated with adsorption were determined from the data in Fig. 5. An estimate of 1300 cal/100 g of solid was obtained for $\Delta H_i(SL)$ by extrapolation of the linear portion of the immersional isotherm to zero moisture content. The integral enthalpy change (column 3 of Table II) was calculated from Eq. 8 by choosing $\Delta H_i(S_fL)$ values from the smooth curve of Fig. 5 at each value for n_1.

As mentioned previously, the differential enthalpy of adsorption was determined by approximating the slope of a plot of ΔH versus n_1 at each n_1 given in Table II. This approximation was performed by determining the slope of a straight-line segment through adjacent experimental values. These values are also included in Table II.

Computation of integral, ΔS, the differential, $\overline{\Delta S}_1$, entropies was performed from the defining equations, Eqs. 9 and 10. Table II includes these values in columns 5 and 8. Figures 8 and 9 are graphical representations of the variation in integral and differential thermodynamic variables throughout adsorption.

Enthalpy Analysis—The integral enthalpy of immersion was characterized by a linear decrease in the heat of wetting throughout the period of low moisture contents. This relationship is consistent with the nearly constant differential enthalpy of adsorption shown in Fig. 9.

The constant differential enthalpy observed in the range of 0–0.15 mole of adsorbate/100 g of solid for microcrystalline cellulose is quite a contrast to the behavior observed in the wetting of standard cellulose (Fig. 10) presented by Morrison and Dzieciuch (11). These authors concluded that
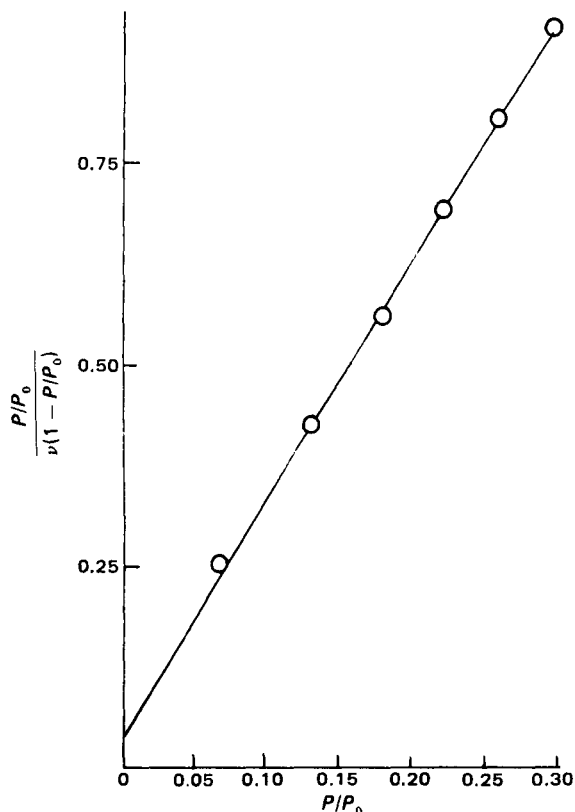
Figure 7—*BET plot for the adsorption of nitrogen by microcrystalline cellulose.*

Figure 9—*Differential thermodynamic properties of the microcrystalline cellulose–water system. Key:* ▲, *differential enthalpy;* ●, *differential entropy;* ■, *differential free energy; and* ν_m, *BET monolayer capacity.*

the initial decrease in the value of $-\overline{\Delta H_1}$ was due to a peptization (swelling) of the solid. The energy consumed in the disruption of solid–solid bonds produced a heat of immersion lower than expected and was not a constant effect. This effect, which is carried implicitly throughout the determination of $\overline{\Delta H_1}$ from immersional data, is not present in the study of microcrystalline cellulose. Therefore, the constant $-\overline{\Delta H_1}$ period seems to be an indication of no swelling as well as an indication of an energetically homogeneous surface.
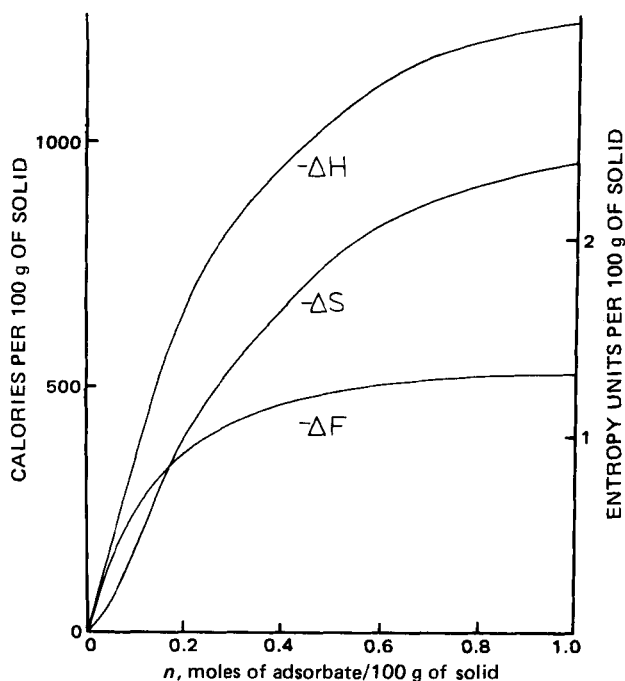

Figure 8—*Integral thermodynamic properties of adsorption for the microcrystalline cellulose–water system.*
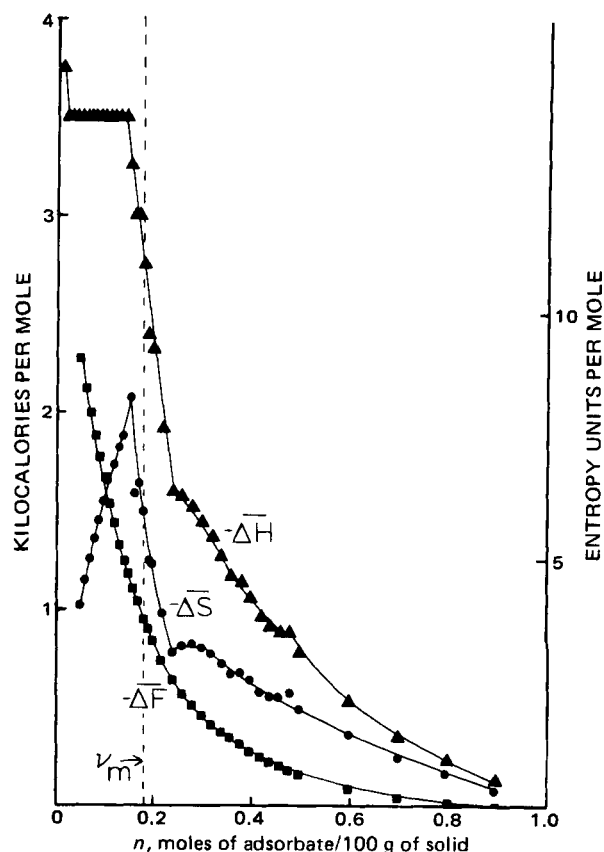
The dashed line in Fig. 9 represents the monolayer capacity as estimated from the BET treatment of the sorption data. Slightly before completion of the monolayer, $-\overline{\Delta H_1}$ begins to decrease rapidly. The end of the constant period indicates the point where lateral adsorbate interactions begin to influence the heat of adsorption. The sharply decreasing values of $-\overline{\Delta H_1}$ seem to indicate the transition from a situation where the majority of water molecules interact by forming two bonds with cellulose to a completed monolayer involving one solid–liquid bond per water molecule.

Values of $\overline{\Delta H_1}$ in Fig. 7 are net values above the heat of condensation to liquid water. A value of $\overline{\Delta H_1} = 0$ indicates that the bonds formed during vapor adsorption have an energy equivalent to the bond strength in liquid water. The heat of condensation of water is approximately -9 kcal/mole; thus, each mole of hydrogen bonds in water has an energy of approximately -4.5 kcal.

At low moisture contents (<0.15 mole of water/100 g of solid), an adsorbed water molecule is likely to form two bonds with the cellulose substrate. In this range, the $\overline{\Delta H_1}$ values of -3.5 kcal/mole represents the bond energy in excess of the normal hydrogen bonds in water: -1.75 kcal/mole of hydrogen bonds. A total hydrogen bond energy between water and cellulose of -6.25 kcal/mole can be calculated by adding the energy for 1 mole of hydrogen bonds in water (-4.5 kcal/mole) to the experimentally measured excess (-1.75 kcal/mole). The inflection point that occurs slightly after ν_m in Fig. 7 has a value of -1.6 kcal/mole. If this entire excess is assigned to the formation of one bond between cellulose and water, a hydrogen bond energy of -6.1 kcal/mole is calculated.

Since the hydrogen bond energy between cellulose and water should be relatively constant despite the orientation of the adsorbed molecule, the closeness of the -6.25- and -6.1-kcal/mole values supports the hypothesis that a partial transition from solid–liquid to liquid–liquid bonding is responsible for the observed decrease in $-\overline{\Delta H_1}$.

The values of -1.75 and -1.6 kcal/mole obtained calorimetrically compare reasonably well to the net interaction energy estimated from the BET theory. The parameter c had a value of 16.48 and, with Eq. 12, this value leads to a net interaction of -1.66 kcal/mole.

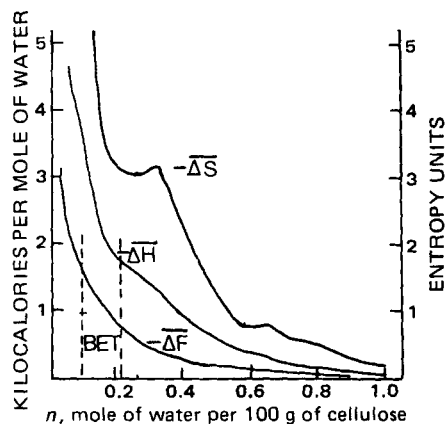**Entropy Analysis**—Entropy represents disorder. Therefore, a neg-

Figure 10—*Net differential enthalpy, free energy, and entropy of adsorption of water by cotton cellulose (adapted from Ref. 11).*

ative change of entropy corresponds to an ordering process. The increase in $-\Delta S$ (Fig. 8) throughout the adsorption process corresponds to an overall increase in the ordering of the system.

The differential entropy curve determined from immersional data reflects the influence of four factors: (a) a decrease in entropy associated with the change of three-dimensional molecular motion to two-dimensional motion (transition effect), (b) an increase in entropy due to the separation of liquid molecules in surface spreading (separation effect), (c) an increase in entropy associated with the disordering or peptization of the solid, and (d) a decrease in entropy associated with ordering in the surface film.

As Wahba (4) indicated, the very early stages of adsorption must always be characterized by a positive differential entropy. This conclusion is a direct result of the fact that while the differential heat of adsorption has a finite value at $P/P_0 = 0$, the differential free energy is infinite (see Eq. 2).

From a conceptual point of view, the positive value of $\overline{\Delta S_1}$ is due to the predominance of the separation effect of liquid molecules. The decrease in this thermodynamic quantity corresponds with the decrease in the separation effect as more molecules are adsorbed. A value of zero for $\overline{\Delta S}$ at low moisture contents does not indicate that the adsorbate is the same as bulk water; it merely represents the point where the separation effect is balanced by the transition from three-dimensional motion to the two-dimensional surface phase.

Generally, experimental free energy values are not available at low relative pressures, so few studies include the $+\overline{\Delta S}$ values of this region. The initial region of the differential entropy curve for the adsorption of water on microcrystalline cellulose (Fig. 9) corresponds to an increase in $-\overline{\Delta S_1}$. This region of the curve is primarily a result of a decrease in the separation effect. In other words, this region corresponds to a period of ordering, due primarily to the approach of monolayer completion. If there were any perturbation of the solid during this period such as swelling, that effect would oppose the experimental results in the sense that the perturbation would represent an increase in entropy.

Ideally, the maximum in $-\overline{\Delta S_1}$ observed around $n = 0.15$ would represent the point where the separation effect reached a minimum and the ordering due to surface packing reached a maximum, *i.e.*, completion of the monolayer. Wahba (4) commented that actually the maximum will occur slightly before monolayer completion because there is undoubtedly some premature multilayer formation. Indeed, in this study, the maximum appears slightly before the monolayer capacity as estimated from adsorption data.

A comparison of the results for standard cellulose, obtained by Morrison and Dzieciuch (11) (Fig. 10), with the results of the microcrystalline cellulose study reveals major differences between these two materials in the low pressure region where the standard cellulose curve does not exhibit a maximum. Morrison and Dzieciuch (11) indicate that the rapid decrease of $-\overline{\Delta S_1}$ is due in part to the disordering of the dried gel and in part to the replacement of two or more hydrogen bonds per water molecule by one per molecule. Peptization of the standard cellulose represents swelling of the fibers and, hence, an increase in entropy. This swelling only occurs in regions where moisture can penetrate, and the entropy change associated with the microcrystalline product was not influenced by such perturbation.

Thus, with microcrystalline cellulose, the decreasing region of $-\overline{\Delta S_1}$ near the BET monolayer capacity is exclusively due to the change from

Table III—Calculated Differential Thermodynamic Properties for the Desorption of Water from Saturated Microcrystalline Cellulose Samples

n, moles of Water/ 100 g of Solid	P/P_0	$-\Delta \overline{H}$, cal/mole	$-\Delta \overline{F}$, cal/mole	$-\Delta \overline{S}$, eu/mole
1.00	0.987	—	—	—
0.90	0.960	145	24	0.41
0.80	0.911	210	55	0.52
0.70	0.858	270	91	0.60
0.60	0.781	460	146	1.05
0.50	0.711	680	202	1.60
0.48	0.685	650	224	1.43
0.46	0.661	650	245	1.36
0.44	0.638	800	266	1.79
0.42	0.615	850	288	1.89
0.40	0.590	825	312	1.72
0.38	0.562	900	341	1.88
0.36	0.535	950	370	1.95
0.34	0.512	1025	396	2.11
0.32	0.480	1225	435	2.65
0.30	0.445	—	—	—

a surface cellulose interaction involving two hydrogen bonds per water molecule to an interaction consisting of one such bond and not to swelling of the solid.

Both standard cellulose (11) and microcrystalline cellulose exhibit a minimum in $-\overline{\Delta S_1}$ around $n = 0.25$, followed by another maximum. This region represents the moisture content where the surface is covered and further adsorption occurs with much less ordering. Since the value of $-\overline{\Delta S_1}$ drops off faster for cellulose than it does for microcrystalline cellulose, the nature of the microcrystalline solid apparently is still influential at higher relative pressures.

Such behavior seems characteristic of the difference between adsorption with a fibrous solid and adsorption involving discrete particles of essentially the same material. Fibers tend to confine the adsorption so that interactions between adjacent layers of adsorbate are inevitable. The immersional data of the cellulose–water system (11) confirm this hypothesis by showing a negligible heat of wetting for saturated solid. In contrast, the heat of wetting of saturated microcrystalline cellulose has been used as a method for estimating the external solid surface area.

Origin of Hysteresis—The strength of the solid–liquid bond plays a role in the origin of hysteresis in the microcrystalline cellulose–water system. Possibly, an increase in enthalpy at a given partial pressure could entirely account for an increase in free energy (see Eq. 10). If so, the entropy of water molecules on the surface of microcrystalline cellulose would be the same regardless of whether the water is adsorbed or remains after partial desorption. Table III contains the calculated differential quantities based upon desorption data. A comparison of these differential entropies with those for adsorbed water (Table II) at the same partial pressures shows that the hysteresis is real and does indeed involve both enthalpic and entropic factors since the $\overline{\Delta S_1}$ values are not identical.

SUMMARY AND CONCLUSIONS

Surface characteristics of powders, especially hydrophilic powders, are not easily characterized through experimental methods such as contact angle measurement or tensile strength determinations. The calorimetric approach represents an almost exclusive and particularly appropriate procedure. Immersion in an aqueous environment is, after all, the ultimate fate of most pharmaceutical dosage forms.

With the calorimetric technique, the following surface characteristics have been quantified for microcrystalline cellulose powder:

1. The solid has a strong affinity for water, demonstrated by a heat of wetting of -13.00 cal/g and monolayer coverage occurring at approximately 20% RH.

2. The surface is energetically uniform, showing a linear decrease in the heat of wetting of samples with adsorbed moisture up to monolayer coverage.

3. The powder is relatively porous with an internal surface area of 130–270 m²/g. This surface area represents at least 95% of the surface that interacts with water. Nitrogen adsorption does not give a reasonable estimate of the total surface area.

4. The powder does not swell during the adsorption or wetting process.

5. Hysteresis of the immersional isotherm indicates that, once wetted, the solid holds water tighter at the same moisture content than when the water is adsorbed by dry solid.

6. Sorption hysteresis is of enthalpic and entropic origin.

The widespread use of microcrystalline cellulose powder in the pharmaceutical industry as a tablet excipient makes this specific information of particular relevance. However, the general experimental procedure represents a technique that has as its greatest potential application the determination of changes in surface characteristics as a result of formulation and/or processing.

REFERENCES

(1) G. E. Boyd and W. D. Harkins, *J. Am. Chem. Soc.*, **64**, 1190 (1942).
(2) W. D. Harkins and G. E. Boyd, *ibid.*, **64**, 1195 (1942).
(3) W. D. Harkins and G. Jura, *ibid.*, **66**, 919 (1944).
(4) M. Wahba, *J. Phys. Colloid Chem.*, **54**, 1148 (1950).
(5) G. J. Young, J. J. Chessick, F. H. Healey, and A. C. Zettlemoyer, *J. Phys. Chem.*, **58**, 313 (1954).
(6) G. J. Young and F. H. Healey, *ibid.*, **58**, 881 (1954).
(7) F. H. Healey and G. J. Young, *ibid.*, **58**, 885 (1954).
(8) A. C. Zettlemoyer, G. J. Young, and J. J. Chessick, *ibid.*, **59**, 962 (1955).
(9) H. B. Dunford and J. L. Morrison, *Can. J. Chem.*, **33**, 904 (1955).
(10) J. L. Morrison and J. F. Hanlan, *Nature*, **179**, 528 (1957).
(11) J. L. Morrison and M. A. Dzieciuch, *Can. J. Chem.*, **37**, 1379 (1959).
(12) Y. C. Wu and L. E. Copeland, *Adv. Chem. Ser.*, No. 33, 357 (1961).
(13) M. Dole and A. D. McLaren, *J. Am. Chem. Soc.*, **69**, 651 (1947).
(14) S. Brunauer, P. H. Emmett, and E. Teller, *J. Am. Chem. Soc.*, **60**, 309 (1938).
(15) S. Brunauer, L. S. Deming, W. E. Deming, and E. Teller, *ibid.*, **62**, 1723 (1940).
(16) W. D. Harkins and G. Jura, *ibid.*, **66**, 1362 (1944).
(17) R. H. Stokes and R. A. Robinson, *Ind. Eng. Chem.*, **41**, 2013 (1949).
(18) J. M. Sturtevant, in "Physical Methods of Organic Chemistry," vol. 1, A. Weissburger, Ed., Interscience, New York, N.Y., 1945, pp. 335–344.
(19) R. G. Hollenbeck, G. E. Peck, and D. O. Kildsig, *J. Pharm. Sci.*, **67**, 1592 (1978).
(20) G. H. Argue and O. Maass, *Can. J. Res.*, **12**, 564 (1935).
(21) J. D. Babbitt, *ibid.*, **20**, 143 (1942).
(22) S. J. Gregg, "The Surface Chemistry of Solids," Reinhold, New York, N.Y., 1951, pp. 24–26.
(23) Y. Nakai, E. Fukuska, S. Nakajima, and J. Hasegawa, *Chem. Pharm. Bull.*, **25**, 96 (1977).
(24) K. Marshall and D. Sixsmith, *Drug Dev. Commun.*, **1**, 51 (1974–75).
(25) F. W. Billmeyer, "Textbook of Polymer Science," 2nd ed., Wiley–Interscience, New York, N.Y., 1971.

Glass Formation in Barbiturates and Solid Dispersion Systems of Barbiturates with Citric Acid

M. P. SUMMERS

Abstract □ Glasses were prepared from a number of barbiturates. The viscosities and glass transition temperatures of the glasses were dependent on the structure of the groups present on the C-5 and N-1 atoms. Solid dispersions were prepared from three selected barbiturates formulated with citric acid. The glass transition temperatures of these systems indicated that a 1:1 molar ratio complex was formed between the two components and that intermolecular bonding was stronger in the complex than in the individual components.

Keyphrases □ Barbiturates, various—glass formation and solid dispersion systems evaluated □ Glass formation—various barbiturates evaluated □ Solid dispersion systems—various barbiturates evaluated □ Central depressants—various barbiturates, glass formation and solid dispersion systems evaluated

The use of citric acid as a glass-forming carrier in solid dispersions was studied previously (1–3). Although the dissolution rate of primidone formulated in such a system was faster than that of the pure drug, the glassy phase of this system was unstable and studies had to be performed on the devitrified solid (2).

To study the full potential of a glass system for improved drug dissolution, it is necessary to find a system with a glass transition temperature well above room temperatures so that a hard, usable glass can be formed. It would probably be advantageous if the drug could exist as a glass, which may stabilize the glass formed by the carrier.

The purpose of the present work was to study glass formation in a series of barbiturates and the formation of binary glass systems with citric acid to find a system that complied with the suggested criteria.

EXPERIMENTAL

Preparation of Barbiturate Glasses and Solid Dispersion Systems—Glass formation was studied in the following barbiturates: barbital[1], mephobarbital[2], phenylmethylbarbituric acid[3], pentobarbital[2], hexobarbital[4], phenobarbital[5], heptabarbital[6], butethal[3], amobarbital[3], ethylpropylbarbituric acid, cyclobarbital, and 5-ethyl-5-cycloheptenyl-1-methylbarbituric acid[6].

---

[1] BDH Chemicals Ltd., Poole, England.
[2] Siegfried, Zofingen, Switzerland.
[3] May and Baker Ltd., Dagenham, England.
[4] Sigma Chemical Co., St. Louis, Mo.
[5] Macarthys, Romford, England.
[6] Geigy Pharmaceuticals, Macclesfield, England.